JVI Journals.ASM.org

Proteolytic Activation of the Porcine Epidemic Diarrhea Coronavirus Spike Fusion Protein by Trypsin in Cell Culture

Oliver Wicht,[a] Wentao Li,[a] Lione Willems,[a] Tom J. Meuleman,[a] Richard W. Wubbolts,[b] Frank J. M. van Kuppeveld,[a] Peter J. M. Rottier,[a] Berend Jan Bosch[a]

Virology Division, Department of Infectious Diseases and Immunology, Faculty of Veterinary Medicine, Utrecht University, Utrecht, The Netherlands[a]; Department of Biochemistry and Cell Biology, Faculty of Veterinary Medicine, Utrecht University, Utrecht, The Netherlands[b]

ABSTRACT

Isolation of porcine epidemic diarrhea coronavirus (PEDV) from clinical material in cell culture requires supplementation of trypsin. This may relate to the confinement of PEDV natural infection to the protease-rich small intestine of pigs. Our study focused on the role of protease activity on infection by investigating the spike protein of a PEDV isolate (wtPEDV) using a reverse genetics system based on the trypsin-independent cell culture-adapted strain DR13 (caPEDV). We demonstrate that trypsin acts on the wtPEDV spike protein after receptor binding. We mapped the genetic determinant for trypsin-dependent cell entry to the N-terminal region of the fusion subunit of this class I fusion protein, revealing a conserved arginine just upstream of the putative fusion peptide as the potential cleavage site. Whereas coronaviruses are typically processed by endogenous proteases of the producer or target cell, PEDV S protein activation strictly required supplementation of a protease, enabling us to study mechanistic details of proteolytic processing.

IMPORTANCE

Recurring PEDV epidemics constitute a serious animal health threat and an economic burden, particularly in Asia but, as of recently, also on the North-American subcontinent. Understanding the biology of PEDV is critical for combatting the infection. Here, we provide new insight into the protease-dependent cell entry of PEDV.

Porcine epidemic diarrhea virus (PEDV) belongs to the genus *Alphacoronavirus* in the family *Coronaviridae* and is the causative agent of porcine epidemic diarrhea (1). The virus is prevalent in East Asia, inflicting severe economic damage due to high mortality rates in young piglets, and recently made its first appearance on the North American subcontinent (2–4). PEDV infects the epithelia of the small intestine, an environment rich in proteases, and causes villous atrophy, resulting in diarrhea and dehydration. Intriguingly, *in vitro* propagation of PEDV isolates requires supplementation of trypsin to the cell culture supernatant (5). It has been hypothesized that trypsin mediates activation of virions for membrane fusion by cleaving the spike (S) glycoprotein (5, 6). Trimeric S proteins decorate the virion envelope and mediate receptor binding and membrane fusion. The S protein has been recognized as a class I fusion protein by its molecular features (7, 8).

Class I fusion proteins are generated in a locked conformation to prevent premature triggering of the fusion mechanism and are subsequently prepared for action by proteolytic processing, a step called priming (reviewed in reference 9). This cleavage is separating two functionally distinct protein domains, a soluble head domain responsible for receptor binding and a membrane bound subunit comprising the fusion machinery. A characteristic feature of the cleaved, fusion-ready subunit is an N-terminal fusion peptide. Proteolytic priming can occur in the virus-producing cell, in the extracellular environment, or after contact with the target cell membrane. Priming of the PEDV S protein is potentially accomplished by intestinal digestive enzymes.

Some coronaviruses (CoV), such as mouse hepatitis virus (strain A59) and infectious bronchitis virus (IBV), carry S proteins that are cleaved by furin-like proteases in the producer cell at the junction of the receptor binding (S1) and the membrane fusion subunit (S2) (10, 11). However, most CoV-like PEDV and severe acute respiratory syndrome coronavirus (SARS-CoV) carry noncleaved S proteins upon release (12). For an increasing number of coronavirus S proteins, an alternative cleavage site within the S2 subunit (S2′) has been described that is located upstream of the putative fusion peptide (13–15). Unlike cell culture-adapted PEDV, clinical isolates of PEDV are the only known CoVs for which propagation in cultured cells is dependent on a protease that is not expressed by target cells. The spatiotemporal and mechanistic characteristics of their fusion activation remain unknown.

We focus our investigation on the impact of trypsin on PEDV S protein by using a reverse genetics system based on the cell culture-adapted, trypsin-independent PEDV strain DR13 (caPEDV) (16, 17). We generated two isogenic recombinant viruses with caPEDV background genes—PEDV-Swt and PEDV-Sca—expressing the S protein of a strictly trypsin-dependent PEDV isolate CV777 and that of caPEDV, respectively (18). Indeed, the trypsin dependency of virus propagation was attributed to the S protein. Trypsin was necessary for efficient cell entry and release of PEDV-Swt, whereas it reduced infection of PEDV-Sca. We demonstrated that trypsin was required for PEDV-Swt entry only after receptor binding. We mapped the genetic determinants

Received 4 February 2014 **Accepted** 23 April 2014
Published ahead of print 7 May 2014
Editor: S. Perlman
Address correspondence to Berend Jan Bosch, b.j.bosch@uu.nl.

doi:10.1128/JVI.00297-14

for activation of the S protein through trypsin to a site just upstream of the putative fusion peptide by testing various chimeric forms of the S genes and specific point mutations.

MATERIALS AND METHODS

Cells and viruses. Vero-CCL81 cells (ATCC) were maintained in Dulbecco modified Eagle medium (DMEM; Lonza catalog no. BE12-741F) supplemented with 10% fetal bovine serum (FBS). A Vero-CCL81-derived cell line expressing the MHV receptor, murine carcinoembryonic antigen-related cell adhesion molecule 1a (CCM), was made by transduction with vesicular stomatitis virus G protein-pseudotyped Moloney murine leukemia virus (MLV) using the pQCXIN retroviral vector (Clontech) containing the CCM coding sequence (19). The polyclonal Vero-CCM cell line was selected and maintained with G418 (PAA), and CCM expression was confirmed by immunostaining. To propagate PEDV, cell layers were generally washed twice with phosphate-buffered saline (PBS), and maintenance medium was substituted by Eagle's minimum essential medium Alpha Modification (Life Technologies catalog no. 22571-020) supplemented with 0.3% tryptose phosphate broth (aMEM-TPB; Sigma catalog no. T9157). The cell culture-adapted PEDV DR13 strain, here called caPEDV (JQ023162; isolated from a commercial vaccine of GreenCross, South Korea), and recombinant virus carrying caPEDV S protein, including trypsin-independent derivatives thereof, were propagated and titrated in aMEM-TPB supplemented with 20 mM HEPES in Vero cells (20). PEDV strain CV777, here called wtPEDV (AF353511; kindly provided by Kristin van Reeth, Ghent University), and recombinant virus carrying wtPEDV S protein or derivatives thereof were propagated and titrated in aMEM-TPB supplemented with 20 mM HEPES and 15 μg/ml trypsin (Sigma catalog no. T4799) in Vero cells. The S gene of wtPEDV encoded two amino acid deviations from the published CV777 S sequence (G84S and S503L [7]). For purification of the PEDV-Swt virus particles in the absence of trypsin, Vero cells were inoculated in the presence of trypsin activity, reaching a maximum infection rate, and the culture supernatant was replenished by aMEM-TPB supplemented with 20 mM HEPES after 4 h. Cells were cultured for 24 h at 37°C and an additional 24 h at 32°C. Virus was harvested by three cycles of freeze-thawing the infected cells and culture supernatant followed by removal of cell debris by centrifugation at 4,000 × *g* for 10 min.

Construction of recombinant viruses. Recombinant PEDVs were generated as described by Li et al. (16), except that we used Vero-CCM cells for the recovery of viruses carrying wtPEDV S protein or trypsin-dependent derivatives thereof. PEDV-Sca represents the earlier reported PEDV-ΔORF3/GFP (where ORF3 is open reading frame 3 and GFP is green fluorescent protein) (16) that was generated using the transfer vector p-PEDV-ΔORF3/GFP. The transfer vectors for novel recombinants were derivatives of p-PEDV-ΔORF3/GFP containing a BamHI restriction site between ORF1b and the S gene, as described for p-rPEDV (16). The chimeric PEDV-S_AB, PEDV-S_Ab, and PEDV-S_aB genes were generated by replacing the PstI × PmlI, PstI × Bsu36I, or Bsu36I × PmlI fragments of the caPEDV S gene with those of the wtPEDV sequence. To generate recombinant PEDV with the full-length wtPEDV S protein (PEDV-Swt), the entire S gene was replaced by BamHI × PmlI, generating p-PEDV-CV777-ΔORF3/GFP. The FLAG peptide (VQDYKDDDDK)-encoding gene fragment was appended to the C-terminal end of the S gene using the PmlI restriction site of p-PEDV-ΔORF3 and p-PEDV-CV777-ΔORF3/GFP, resulting in PEDV-Sca_flag and PEDV-Swt_flag, respectively (16). Viral RNA was extracted from virus two to three passages after plaque selection, and the genotype was confirmed by sequencing.

Infection/virus entry assay. Vero cells were inoculated with caPEDV and wtPEDV (multiplicity of infection [MOI] was set to 0.1 in the presence of trypsin) in the presence of 15 μg/ml trypsin or trypsin and 40 μg/ml soy bean trypsin inhibitor type I (SBTI; Sigma catalog no. T6522) for 15 h before visualization of the virus infection by immunofluorescence microscopy. For recombinant PEDV containing the GFP reporter gene (MOI was set to 0.1 in the presence of trypsin), inocula contained 15 μg/ml trypsin, 40 μg/ml SBTI, or both. After 2 h, inoculum was removed, and cell layers were rinsed with PBS and further incubated with aMEM-TPB supplemented with SBTI. Ten to 12 h postinfection, when GFP signals became apparent, samples were imaged by an EVOS-fl fluorescence microscope (Advanced Microscopy Group) and prepared for flow cytometry analysis. Figures show representative images. The same procedure was used if the inoculum had been pretreated. Prior to infection, trypsin or trypsin and SBTI were added to the inoculum and incubated for 1 h at 37°C, followed by inoculation of Vero cells for 2 h. The attachment assay was performed (MOI was set to 0.5 in the presence of trypsin before pretreatment) with pretreated or naive virus preparations, while residual trypsin activity was blocked in all cases by an excess of SBTI. Next, the inoculum was allowed to attach to the cells at ~8°C for 1 h before the cell layer was rinsed, followed by 2 h of inoculation with trypsin or trypsin and SBTI. Samples were otherwise prepared as described for the entry assay.

Flow cytometry. The cell layer was rinsed with PBS and detached with cell culture dissociation solution (Sigma catalog no. C5914). Cells were resuspended in PBS supplemented with 2% FBS and 0.02% sodium azide, pelleted by centrifugation, and fixed in 3.7% formaldehyde in PBS. Subsequently, cells were analyzed for GFP expression using a FACSCalibur flow cytometer (BD Bioscience) recording 20,000 cells. Flowing software 2 (Perttu Terho, Turku Centre for Biotechnology, Finland) was used to analyze the percentage of GFP-expressing cells in the live cell gate. The threshold for mock-infected cells was set at 0.1% positive cells.

Virus release assay. To assess the release of infectious particles in the absence or presence of trypsin, Vero cells were inoculated with recombinant PEDV at an MOI of 4 for 2 h and further incubated in aMEM-TPB or aMEM-TPB supplemented with 15 μg/ml trypsin. Fourteen to 16 h postinfection, supernatant was collected, and cell debris was removed by spinning for 10 min at 10,000 × *g* and pretreated with 15 μg/ml trypsin for 1 h before titration of infectious virus by endpoint dilution. The trypsin pretreatment was performed to ensure equal trypsin-induced reduction of PEDV-Sca infectivity of samples obtained under different conditions. To display the data, ratios of viral titers obtained from supernatants containing trypsin versus lacking trypsin were calculated for paired samples. The *P* value was obtained with a paired-sample *t* test between PEDV-Swt and PEDV-Sca.

The effect of trypsin on the release of viral RNA in the cell culture supernatant was determined by quantitative real-time reverse transcription-PCR (qRT-PCR). Vero cells were inoculated with recombinant PEDV at an MOI of 2 for 2 h and further incubated in aMEM-TPB supplemented with 40 μg/ml SBTI or 15 μg/ml trypsin. Sixteen hours postinfection, RNA was prepared from cell lysates (RNeasy minikit; Qiagen) and cell culture supernatants (QiaAMP viral RNA minikit; Qiagen) according to the manufacturer's protocols. Reverse transcription and qRT-PCR were performed using GoTaq 1-Step qRT-PCR system (Promega catalog no. A6020) with the primer set forward 5′-GAGCACATGTTGTTGGCTCT-3′ and reverse 5′-GCAACCTTCAGGTCTGACAA-3′ on a Light Cycler 480 II (Roche).

PEDV S protein expression vectors. cDNA was recovered from virus preparations, and wtPEDV S gene-specific PCR products were subcloned into pCAGGS expression vector for transient expression (Swt). To increase cell surface presentation during transient expression, the C terminus of the S gene was truncated by an equivalent of 20 amino acids, which included retrieval signals (21). The point mutation R890G was introduced to the wtPEDV S gene by site-directed mutagenesis (Swt_R890G). The entire S protein coding sequence of each construct was confirmed by sequencing.

PEDV S protein-mediated cell-cell fusion. Vero cells were transfected with pCAGGS expression plasmids encoding Swt or the Swt_R890G mutant using jetPRIME (Polyplus) for 48 h. Alternatively, Vero cells were inoculated with PEDV-Swt for 2 h in the presence of trypsin and cultured from 2 to 20 h in the absence of trypsin. Supplementation of 15 μg/ml trypsin for 1 h resulted in cell-cell fusion, which was monitored by immunofluorescence staining against PEDV S protein in the case of overexpres-

sion. Cell-cell fusion of cells infected with the GFP-expressing PEDV-Swt was followed by real-time confocal fluorescence microscopy using a NIKON A1R microscope with a top climate chamber (Tokai Hit) for live cell imaging at 37°C and 5% CO_2. Image stacks were acquired every 65 s at ×40 magnification.

Immunofluorescence microscopy. For immunostaining, the cells were washed twice with PBS and fixed with 3.7% formaldehyde (Merck catalog no. 1040031000) in PBS, followed by membrane permeabilization with 0.1% Triton X-100 (Sigma catalog no. 93426) in PBS for 15 min at room temperature. Cells were blocked by 2% normal goat serum in PBS for 1 h and then incubated with polyclonal rabbit antibody raised against the PEDV (strain D24) S1 ectodomain (amino acids 1 to 728, anti-PEDV-S1 serum; Davids Biotechnologie GmbH, Germany) or the 3F12 mouse monoclonal antibody detecting PEDV nucleocapsid protein (BioNote, Republic of Korea) for 1 h. After cells were rinsed three times with PBS, staining was completed by goat α-rabbit Alexa Fluor488-conjugated (Life Technologies catalog no. A11008) or goat α-mouse Alexa Fluor488-conjugated (Life Technologies catalog no. A11001) antibody. For nuclear staining, 4′,6-diamidino-2-phenylindole (DAPI) (Molecular Probes) was included during blocking. An EVOS-fl fluorescence microscope (Advanced Microscopy Group) was used to visualize staining.

Western blot analysis. Viruses containing cell culture supernatants were purified and concentrated (factor of 1:400, vol/vol) by sedimentation of the virus particles through a 20% cushion of sucrose in HCN buffer (50 mM HEPES, 100 mM NaCl, 10 mM $CaCl_2$) at 100,000 × *g* for 1.5 h at 4°C. Virus particles were handled on ice and resuspended in HCN buffer. For trypsin treatment, samples were supplemented with or without 15 μg/ml trypsin before being warmed to 37°C for 30 min. Samples were chilled and trypsin activity was quenched by the addition of 80 μg/ml SBTI before the titers were determined by endpoint dilution or denaturing in Laemmli sample buffer at 95°C for 10 min. Samples were subjected to sodium dodecyl sulfate-polyacrylamide gel electrophoresis (SDS-PAGE) in a discontinuous gel with 8% acryl amide in the separating gel. Next, samples were transferred to a polyvinylidene fluoride membrane (Bio-Rad catalog no. 162-0176) and blocked with bovine serum. PEDV S protein was reacted with mouse monoclonal anti-FLAG conjugated to horseradish peroxidase (Sigma catalog no. A8592) or anti-PEDV-S1 serum in PBS with 5% FBS and 0.5% Tween 20 and the latter subsequently with swine anti-rabbit immunoglobulin G-conjugated horseradish peroxidase (Dako catalog no. P0217). For detection, we used the Amersham ECL Western Blotting Analysis System (GE Healthcare catalog no. RPN2109) with X-Omat LS films (Kodak; Sigma catalog no. F1149).

Computational analysis. The transmembrane domain of PEDV S protein was predicted by TMHMM 2.0 and the signal peptide by SignalP 4.1. HR1 and HR2 regions are drawn according to Bosch et al. (8). Microscopy images were quantified with ImageJ and GIMP. Amino acid sequence alignment was performed by ClustalW2 using S sequences of PEDV-DR13-par (parental virulent strain DR13, AFE85962.1), Middle East respiratory syndrome coronavirus (MERS-CoV strain HCoV-EMC, AFS88936.1), SARS-CoV strain Tor2, NP_828851.1), IBV (strain Beaudette, NP_040831.1), and murine hepatitis virus (MHV strain A59, NP_045300.1).

RESULTS

***In vitro* infection with PEDV strains CV777 and caDR13.** The requirement for trypsin for the propagation of the PEDV isolate CV777 (wtPEDV) and the cell culture-adapted DR13 strain (caPEDV) was compared. Vero cells were inoculated with either of the two viruses in the absence or presence of trypsin for 15 h. Virus-infected cells were visualized by immunofluorescence staining. Numerous multinucleated cells were observed after inoculation with wtPEDV and caPEDV in the presence of trypsin (Fig. 1). These syncytial foci, typical for PEDV infection (5), were larger for wtPEDV than for caPEDV. In contrast, when trypsin activity was blocked using soy bean trypsin inhibitor (SBTI), wtPEDV infection was almost absent. caPEDV continued to infect cells, even at a higher rate. Remarkably, no syncytium formation was observed in the absence of trypsin activity.

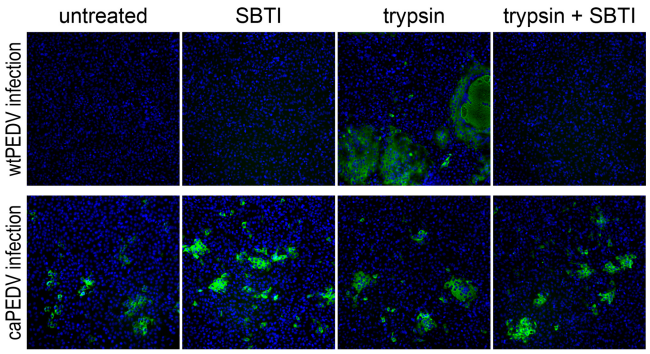

FIG 1 Infection with the wild-type PEDV isolate but not with cell culture-adapted PEDV benefits from trypsin activity. Inocula were supplemented with soy bean trypsin inhibitor (SBTI), trypsin, or a combination of both and applied to Vero cells. After 15 h of incubation, infected cells were detected by immunofluorescence staining against the nucleocapsid protein (green). Nuclei were stained with DAPI (blue).

Recombinant PEDV with different S proteins. Assuming that the addition of trypsin to the inoculum might activate viral S proteins for fusion, we investigated this possible relationship further. We generated recombinant viruses encoding the wtPEDV S gene (PEDV-Swt) or the caPEDV S gene (PEDV-Sca) in an isogenic background, the viruses hence only differing in their S proteins (Fig. 2A). In the recombinant viruses, the ORF3 was replaced by a GFP gene to enable the detection of infection by fluorescence (16). Recovery and propagation of recombinant PEDV-Swt, but not that of PEDV-Sca, required the presence of active trypsin during inoculation and culturing. We concluded that the contrasting trypsin dependence of wtPEDV and caPEDV was determined by the S protein.

Trypsin affects different steps in the viral life cycle. Trypsin might affect virus propagation at different steps in the viral life cycle. First, we focused on virus entry. Vero cells were inoculated in the presence of trypsin for 2 h with PEDV-Sca or PEDV-Swt at an MOI known to infect about 10% of cells. For additional samples, trypsin activity was quenched by the addition of SBTI or only SBTI was added. After the virus entry stage, the inoculum was removed and incubation was continued in the presence of SBTI for 9 h to prevent syncytium formation by residual trypsin in the culture supernatant. At 11 h postinfection (p.i.), fluorescence microscopy images were acquired. Inoculation with PEDV-Swt and PEDV-Sca in the presence of trypsin yielded ~10% infected cells (Fig. 2B). However, in the absence of trypsin activity, PEDV-Swt failed to infect Vero cells. SBTI alone had the same effect as when combined with trypsin. In contrast, inoculation with PEDV-Sca was more efficient without trypsin activity. No syncytia were observed with either recombinant virus in the absence of trypsin. Prolonged incubation in the absence of trypsin activity resulted in second-round infections by PEDV-Sca but not by PEDV-Swt (data not shown). GFP-expressing cells were quantified by flow cytometry to determine the extent of infection. Blocking active trypsin resulted in a >10-fold reduction of PEDV-Swt infection, where we observed a 3-fold increase of infection for PEDV-Sca (Fig. 2C). Thus, PEDV-Swt entry was clearly dependent on active trypsin, whereas PEDV-Sca was not.

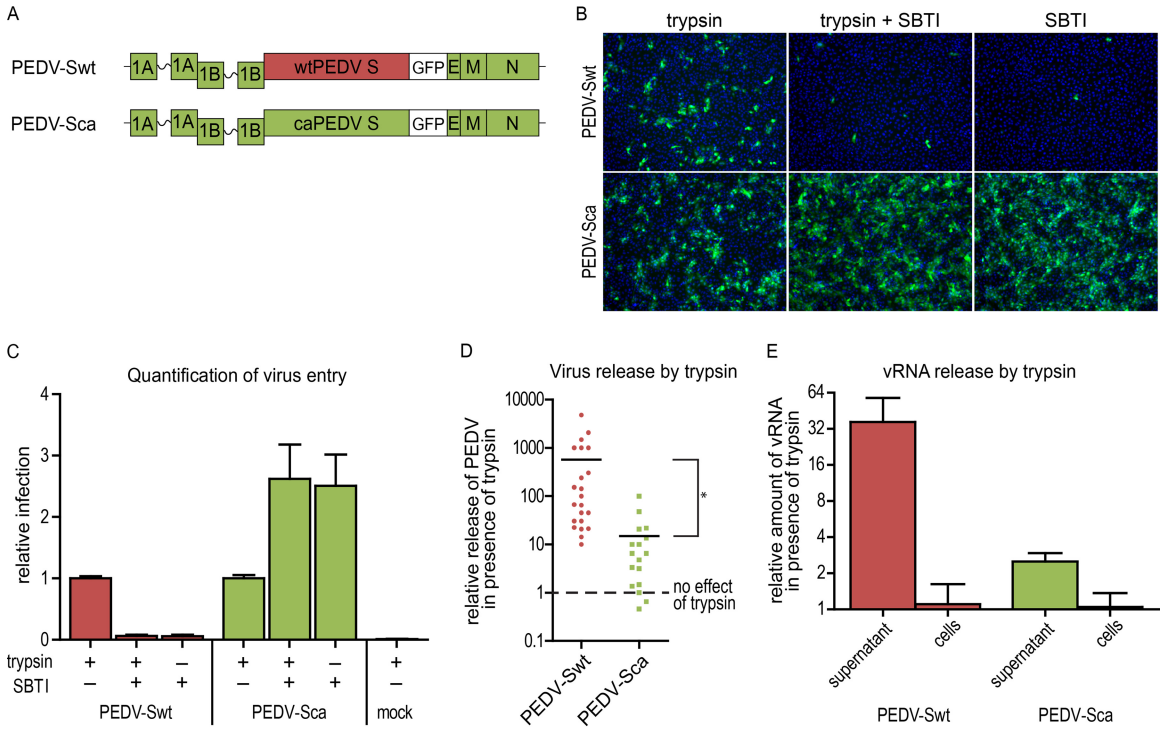

FIG 2 The S protein determines trypsin dependency of PEDV propagation. (A) Schematic representation of the recombinant PEDV genomes carrying the PEDV-CV777 or the PEDV-caDR13 S gene in the isogenic background of caDR13 (PEDV-Swt and PEDV-Sca, respectively). The ORF3 gene was substituted by a GFP sequence. (B) Vero cells were inoculated in the presence or absence of trypsin or soy bean trypsin inhibitor (SBTI). After 2 h, the inoculum was removed and incubation continued in the presence of SBTI to prevent syncytium formation. At 11 h postinfection (p.i.), infected cells were examined by GFP expression using fluorescence microscopy (green). Nuclei were stained with DAPI (blue). (C) The percentage of infected cells was determined by quantifying GFP-expressing cells using flow cytometry. The averages with standard deviations (SD) from 4 experiments are displayed relative to the inoculation in the presence of trypsin. (D) To assess the effect of trypsin on the release of infectious PEDV particles from producer cells, inoculations were performed for 2 h before the medium was refreshed, and incubation was continued in the absence or presence of trypsin. At 14 to 16 h p.i., supernatants were collected. Trypsin was added to all samples 1 h before infectious virus titers were determined by endpoint dilution. The ratios of infectivity in samples obtained in the presence/absence of trypsin were calculated and displayed (*, P value of 0.026 in paired-sample t test). Seven independent experiments with multiple replicates were carried out, and each dot represents the ratio obtained from one pair of samples. (E) The effect of trypsin on the release of viral RNA (vRNA) from PEDV-infected cells was quantified. Vero cells were infected with wtPEDV and caPEDV and cultured from 2 to 16 h p.i. in the presence or absence of trypsin. RNA was subsequently purified from supernatants or cells, and vRNA levels were quantified by qRT-PCR. The relative amounts of vRNA of the samples treated with trypsin compared to the samples treated with SBTI are displayed.

Besides enhancing its entry, trypsin has been reported to increase the release of PEDV from infected cells (22). We therefore monitored release of PEDV-Swt and PEDV-Sca in the absence or presence of trypsin. Vero cells were inoculated with PEDV-Swt and PEDV-Sca (MOI = 4), and the inoculum was removed after 2 h. Incubation was continued in the absence or presence of trypsin until 14 to 16 h p.i., after which cell culture supernatants were collected. Trypsin was added to all samples to normalize the trypsin sample conditions before determining viral infectivity in the cell culture supernatant by endpoint dilution assay. For both viruses, more infectious virus was detected in the presence than in the absence of trypsin (Fig. 2D). However, while for PEDV-Swt this increase was ~500-fold, for PEDV-Sca it was limited to ~15-fold. Statistical testing confirmed a significant difference between the increased release of infectious PEDV-Swt over PEDV-Sca from infected cells in the presence of active trypsin. The trypsin-enhanced release of virions in cell culture supernatant was confirmed by determining the ratio of released viral RNA in the presence compared to the absence of trypsin using quantitative real-time reverse transcription-PCR (Fig. 2E).

Characterization of S protein activation. To facilitate virus entry, trypsin may act on the S protein or the target cells, for example on the virus receptor. In a modified entry assay, either the virus or the target cell monolayer was exposed to trypsin for 60 min prior to inoculation. Trypsin activity was quenched by SBTI before or after preincubation or after 2 h of inoculation. Flow cytometry analysis demonstrated that infection by PEDV-Swt was not enhanced by trypsin pretreatment of the inoculum or the cells (Fig. 3A), but trypsin was required during inoculation. Similarly, infection with PEDV-Sca did not benefit from trypsin pretreatment of virus or cells. Rather, exposure to active trypsin reduced PEDV-Sca infectivity in the absence of cells and during inoculation, though it did not inactivate the virus entirely.

We performed Western blot analysis to study effects of trypsin on the S proteins decorating virus particles. To facilitate monitoring of S proteins, recombinant PEDV-Sca_flag and PEDV-Swt_flag were generated in which the S proteins were C-terminally extended by a FLAG-tag. To avoid trypsin exposure during production of PEDV-Swt_flag, we inoculated Vero cells at a high MOI in the presence of trypsin and replaced the cell supernatant with culture medium without trypsin after 4 h. Virus particles were collected from the cell culture supernatants by sedimenta-

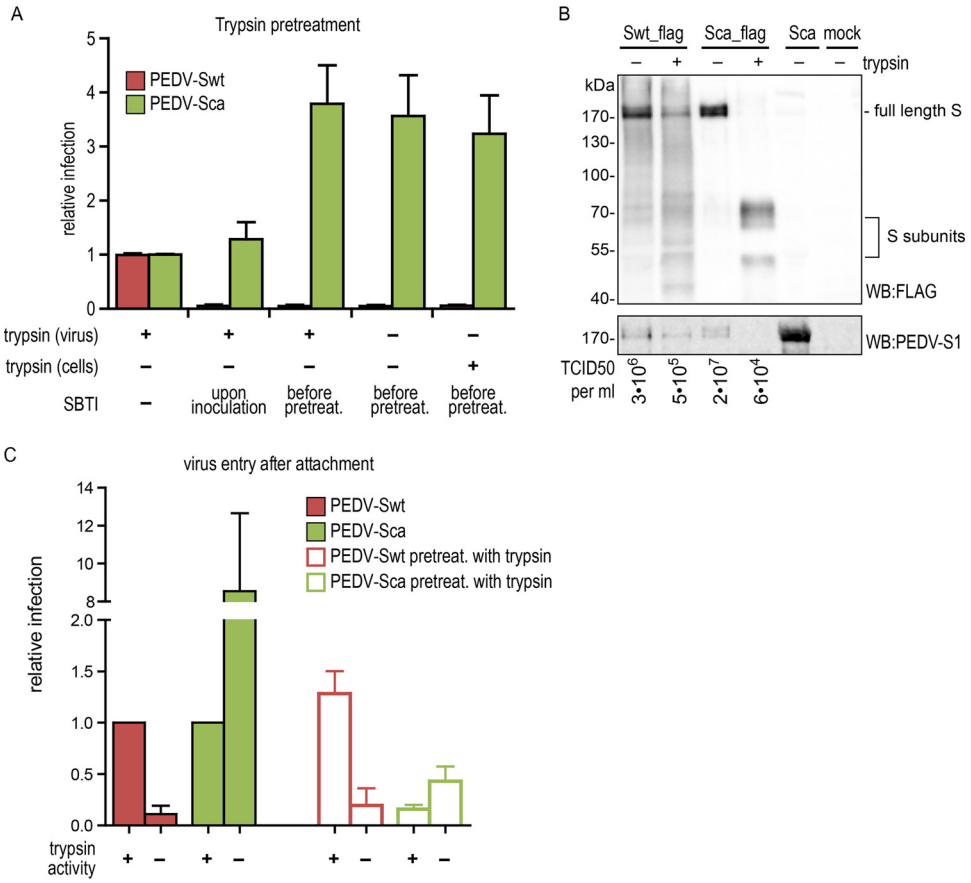

FIG 3 Characterization of S protein activation. (A) An entry assay was performed as described in Fig. 2B. Vero cells were inoculated for 2 h with PEDV-Sca or PEDV-Swt, and infection was quantified by flow cytometry, showing the averages with SD from 3 experiments displayed relative to the inoculation in the presence of trypsin. For pretreatment, the inoculum or the target cells were exposed to trypsin for 1 h at 37°C. SBTI was supplemented to quench the trypsin activity at the indicated steps. (B) Trypsin treatment of S protein on purified virions. Recombinant viruses carrying a FLAG tag at the C terminus of the PEDV-S protein (PEDV-Sca_flag and PEDV-Swt_flag) were produced in the absence of trypsin and purified by pelleting through 20% sucrose. A similar purification procedure was done with culture medium from PEDV-Sca and mock-infected Vero cells (mock). Samples were exposed to 15 μg/ml trypsin or left untreated for 30 min. Infectivity was determined by endpoint dilution (50% tissue culture infective dose [$TCID_{50}$]/ml), and virus particles were subjected to Western blot analysis. Proteins were detected by a mouse monoclonal anti-FLAG antibody conjugated with horseradish peroxidase or rabbit anti-PEDV-S1 serum. (C) Virus supernatant was pretreated as described above with SBTI (filled bars) or trypsin (open bars). After addition of an excess SBTI, virus was added to cells and attachment was allowed for 1 h at 8°C in the absence of trypsin activity. After binding, an entry assay was performed as described for Fig. 2B. Infection was quantified by flow cytometry, showing the averages with SD from 4 experiments displayed relative to inoculation in the presence of trypsin without pretreatment.

tion through a 20% sucrose cushion. Purified virus samples were exposed to 15 μg/ml trypsin for 30 min before Western blot analysis and infectious titer determination. In the absence of trypsin, full-length PEDV S proteins migrating at ~180 kDa were detected using anti-FLAG antibody or an anti-PEDV-S1 serum (Fig. 3B), whereas nontagged PEDV-Sca was detected only by anti-S1 serum. Incubation with trypsin cleaved a fraction of PEDV-Swt but essentially all of PEDV-Sca S protein, resulting in two smaller S protein products that migrated at approximately 70 kDa and 50 kDa. The infectivity of PEDV-Swt_flag and PEDV-Sca_flag decreased by 6-fold and >300-fold, respectively. Thus, the extent of trypsin-mediated proteolysis of the S proteins correlates with the observed reduction of virus infectivity. While PEDV-Swt_flag was relatively resistant to trypsin, PEDV-Sca_flag was rapidly cleaved.

To further define whether trypsin acts before or after receptor binding, we performed a synchronized infection by allowing the viruses to attach to target cells at 8°C in the absence of trypsin. After 60 min, unbound virus was removed and an entry assay was performed. PEDV-Swt was able to infect cells exclusively when trypsin activity was present after attachment (Fig. 3C, filled bars). Trypsin consistently reduced PEDV-Sca infection whenever present. Nonetheless, we assumed that also PEDV-Sca requires proteolytic activation of its S protein at some stage, but that the beneficial cleavage effect of trypsin might be masked by destructive ones. To probe for a trypsin-resistant fraction of PEDV-Sca, virus preparations were pretreated with trypsin or SBTI for 60 min. Then, trypsin was blocked by an excess of SBTI followed by attachment and subsequent infection as before. In contrast, infection by preexposed PEDV-Sca was reduced below the level of infection in the presence of trypsin (Fig. 3, compare filled and empty bars), and the remaining infectivity was further decreased by applying trypsin after attachment. The infectivity of pretreated PEDV-Swt was essentially unaffected and required trypsin activity after attachment. Whereas PEDV-Swt fully depends on trypsin at a post-receptor binding stage, the infectivity of PEDV-Sca is compromised before and after receptor binding.

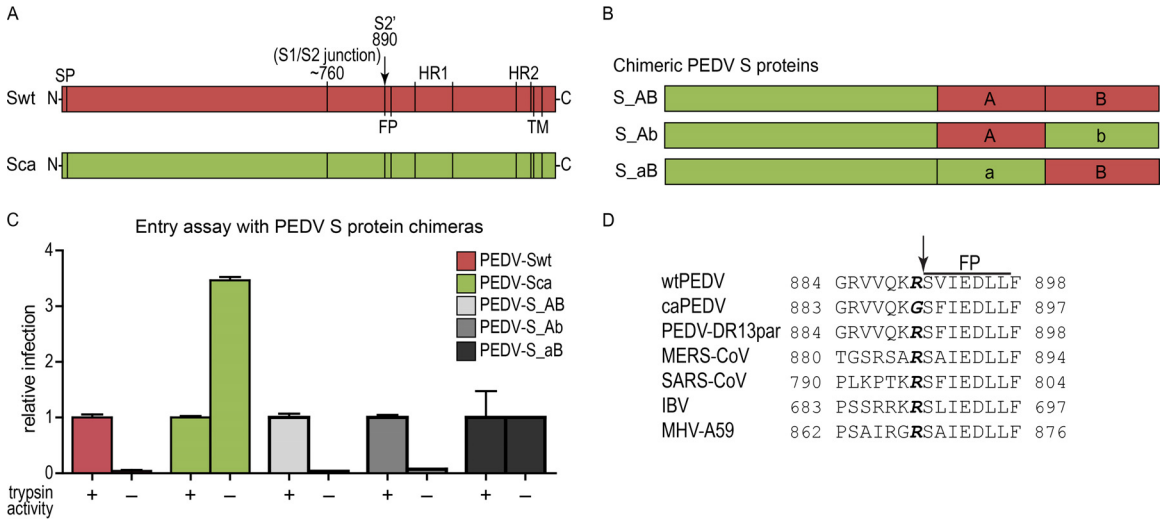

FIG 4 Mapping the genetic determinant for trypsin-enhanced PEDV entry. (A) Putative organization of class I fusion protein features in PEDV S protein. SP, signal peptide; FP, fusion peptide (S891-V910); HR1 and HR2, heptad repeat regions; TM, transmembrane domain; S1/S2 junction, region of the furin cleavage site in MHV-A59; S2′, location of putative cleavage site within the S2 subunit in SARS-CoV and IBV S protein; drawn to scale. (B) A schematic overview shows the chimeric S proteins of the recombinant PEDV variants. Red and green regions are derived from Swt or Sca protein, respectively. (C) An entry assay was performed as described in Fig. 2 to compare the trypsin-dependent entry of PEDV variants. (D) The alignment of the amino acid sequence N-terminal of the fusion peptide (FP) depicts a conserved arginine or a glycine substitution (bold italic). Putative S2′ cleavage site is indicated with an arrow.

Mapping genetic determinants of trypsin-dependent entry. The amino acid sequences of PEDV-Sca and PEDV-Swt differ at 129 amino acid positions. Using a gain-of-function approach, we aimed to map the genetic determinant for trypsin-enhanced entry through substituting fragments of the PEDV-Sca S gene by the corresponding wtPEDV S gene sequences, generating chimeric S proteins. The ultrastructural organization of PEDV S proteins is unknown, but putative functional domains can be identified by theoretical analysis and comparison to other coronaviruses (Fig. 4A). We replaced the gene fragment encoding the putative fusion subunit (PEDV-S_AB), or its N-terminal part containing the putative S2′ cleavage site, fusion peptide, and HR1 domain (PEDV-S_Ab), or its C-terminal part containing HR2, the transmembrane domain, and the C terminus (PEDV-S_aB) (Fig. 4B). Recombinant PEDV-S_AB and PEDV-S_Ab were recovered in the presence of trypsin, whereas PEDV-S_aB could be recovered without trypsin. The chimeric viruses were tested for trypsin-dependent entry as described for Fig. 2. Clearly, all viruses carrying part A of wtPEDV, as exemplified by PEDV-S_AB and PEDV-S_Ab, were found to be fully dependent on trypsin for efficient entry, similar to PEDV-Swt (Fig. 4C). All other viruses that contain part A of caPEDV, such as PEDV-S_aB, did not require trypsin for efficient entry. Hence, part A contains the determinant for trypsin-dependent entry.

To identify the relevant trypsin cleavage site, we compared the amino acid sequences of part A from the PEDV strains CV777 and caDR13 and the parental DR13 virus (PEDV-DR13par). We observed 9 amino acid differences, including one conspicuous arginine, located at position 890 (R890). The arginine occurred in the S protein of wtPEDV and PEDV-DR13par but was replaced by a glycine in the cell culture-adapted caPEDV (Fig. 4D). To investigate the role of R890 in trypsin-mediated entry of wtPEDV, attempts were made to generate PEDV-Swt encoding an R890G substitution. Despite multiple efforts, this virus could not be recovered by our RNA recombination approach, whereas control recombinations were successful (data not shown). We did not consider introducing the reciprocal G890R substitution in PEDV-Sca, since the resulting recombinant virus would be predicted to remain trypsin independent, similar to PEDV-S_aB.

Trypsin-induced cell-cell fusion mediated by overexpressed S proteins. To otherwise assess the role of R890 in trypsin-mediated S protein activation, we made use of a cell-cell fusion assay. As indicated in Fig. 1, continuous treatment of PEDV-infected cells with trypsin results in cell-cell fusion yielding syncytia. Cell-cell fusion was also triggered after overnight infection by addition of trypsin, after which fusion activity continued for more than 1 h (Fig. 5A). To test the trypsin-induced cell-cell fusion capacity of the PEDV S proteins, we transiently expressed them in Vero cells for 48 h. Cell-cell fusion by Swt was compared to that of the Swt_R890G mutant, containing a point mutation substituting the arginine 890 by a glycine. Trypsin was added for 1 h and syncytium formation examined. Trypsin induced considerable syncytia in Swt-expressing cells; in contrast, only small syncytia were induced in the cells expressing Swt_R890G (Fig. 5B). Overexpression of Sca results in small-sized syncytia, and the Sca mutant bearing the reciprocal G890R mutation did not differ in its ability to induce syncytium formation (data not shown). S proteins were stained by immunofluorescence using anti-PEDV-S1 serum, and the sizes of the foci were quantified by counting the number of nuclei (Fig. 5C). For Swt, about 50% of syncytia were found to be small, containing 1 to 4 nuclei, ~25% were medium size, with 5 to 8 nuclei, and ~25% were large, having more than 8 nuclei. In contrast, the Swt_R890G mutant yielded almost 80% of small syncytia, 15% medium, and only 5% large. In both cases, incubation with trypsin failed to trigger syncytium formation by all transfected cells. Of note, the number of small syncytia is probably an overestimate because they were not distinguishable from small clusters of PEDV-S-positive cells originating from cell division.

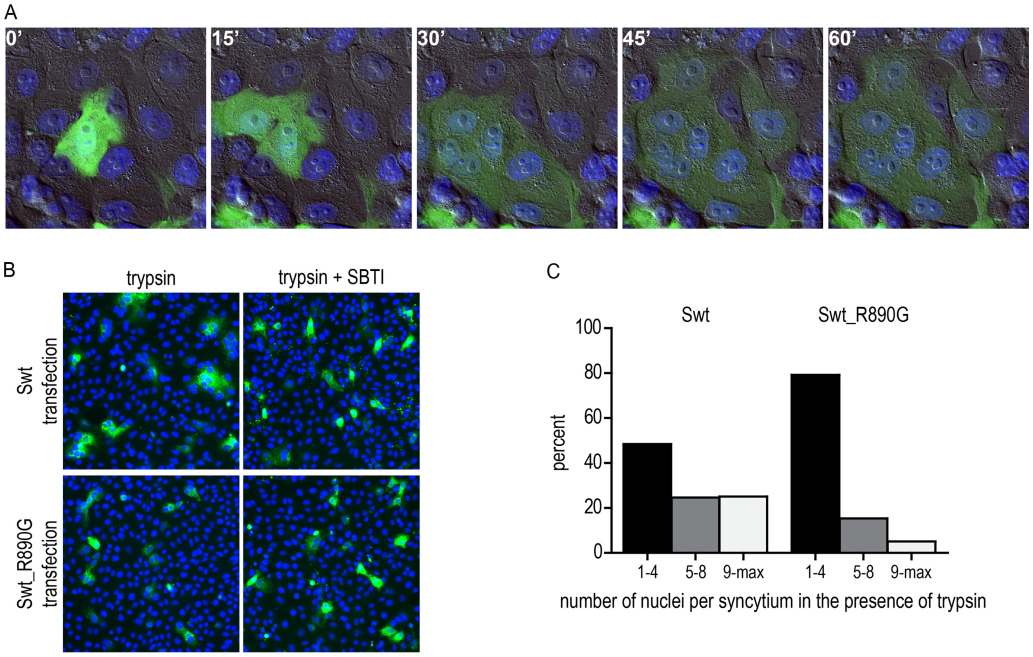

FIG 5 Substitution of arginine at position 890 results in reduced syncytium formation capacity of transiently expressed S protein. (A) After overnight incubation with PEDV-Swt, infected cells were treated with trypsin for 1 h while live images were obtained. Representative images are shown. (B) Vero cells were transiently transfected with expression plasmids encoding Swt and its point mutant Swt_R890G for 48 h. Cells were treated with trypsin or trypsin and SBTI for 1 h and subsequently examined by immunostaining against S protein (green). Nuclei were stained with DAPI (blue). Representative images are shown. (C) The numbers of nuclei per focus were quantified and displayed as binned frequency distribution histogram (four independent experiments, Swt $n = 390$, Swt_R890G mutant $n = 330$). Syncytia containing 1 to 4 nuclei were small, 5 to 8 nuclei were medium, and more than 8 nuclei were large. The average syncytium sizes induced by Swt and Swt_R890G mutant significantly differ from each other (P value of <0.0001, nonparametric t test).

DISCUSSION

Proteolytic priming of class I fusion glycoproteins has been reported to occur with different timing and by various host proteases. Human immunodeficiency virus Env and hemagglutinin (HA) of highly pathogenic influenza viruses become primed by cellular furin-like proteases in the virus-producing cells, hence they are fusion-ready upon virus release (23, 24). In contrast, the infectivity of viruses carrying uncleaved fusion proteins, such as severe acute respiratory syndrome (SARS) coronavirus and low-pathogenic influenza viruses, relies on host cell proteases like type II transmembrane serine proteases (TTSPs) (25), furin-like proteases, or low-pH-dependent endolysosomal proteases (23, 26–28). Recent progress illustrates that infection by respiratory syncytial virus, despite its carrying a cleaved F protein, can still be blocked by inhibitors of endosomal proteases, as the F protein requires a second cleavage in the target cell (29). PEDV is peculiar because it needs an exogenous protease for propagation in cell culture, thereby providing an excellent model to study proteolytic activation. Our investigation of the spatiotemporal characteristics of trypsin-dependent PEDV infection demonstrated that PEDV-Swt undergoes trypsin activation at a post-receptor-binding stage. In contrast to influenza virus HA that can be primed at any stage, we suggest that PEDV S protein is protected from premature processing by reduced accessibility of the cleavage site. This mechanism may prevent premature triggering of the fusion machinery in the protease-rich intestine and help to direct the infection to proper target cells. Proteolytic processing after preconditioning has been observed for other CoVs and correlated with conformational changes that expose a cleavage site. A preceding cleavage of SARS-CoV S protein facilitates cleavage at a second site further C-terminal of the first (30). Like PEDV, MHV-2 S protein requires receptor binding before the cleavage occurs that enables the refolding into a postfusion conformation (31). We failed to observe effects of porcine amino peptidase N (pAPN), the putative receptor for PEDV (32), because we could not reproduce its receptor function in a variety of assays. Proteolytic processing may constitute a general mechanism to control timing and location of the fusion competence of class I fusion proteins. In fact, the tropism of various enveloped viruses, such as low-pathogenic influenza virus, SARS-CoV, human coronavirus 229E, infectious bronchitis virus (IBV), and feline infectious peritonitis virus (FIPV), but also of the nonenveloped rotavirus, has been correlated with the availability of proteases that mediate fusion activation in the target tissue (28, 33–38).

We used recombinant viruses to attribute specific effects of trypsin to the S protein. For the first time, the function of a strictly trypsin-dependent S protein from a PEDV isolate was characterized and compared to the trypsin-independent S protein of a cell-adapted PEDV variant. A previous study claimed that trypsin exerts its PEDV infection-enhancing effect at a post-receptor-binding stage (6). However, the PEDV strain used was not trypsin dependent, and the impact of trypsin on virus propagation was marginal, jeopardizing the interpretation of the data (6, 39).

In search for the genetic determinant of PEDV cleavage, we created viruses with chimeric S proteins by transferring wtPEDV S gene fragments into the trypsin-independent caPEDV virus. We mapped the trypsin dependence feature to the N-terminal half of the fusion subunit, which includes the putative fusion peptide and

HR1 domain (40). A sequence comparison of PEDV S proteins pointed at an arginine (R890)-to-glycine substitution that has occurred during the serial *in vitro* passaging process, which rendered the original parental PEDV-DR13 trypsin independent (41). This arginine was first identified by Belouzard and coworkers (30) in SARS-CoV S protein, and sequence alignment by Yamada et al. (14) illustrated the conservation of this arginine in almost all CoV S proteins. Recombinant PEDV carrying the wild-type S protein encoding the amino acid mutation R890G could not be rescued, suggesting that R890 is required for proper functioning of the S protein. Although we were not able to demonstrate trypsin cleavage at R890 biochemically (data not shown), a role of this residue in trypsin-mediated activation of fusion was indicated by the significant reduction in syncytium formation by cells expressing the CV777 S protein encoding the R890G mutation. R890 is located immediately adjacent to the putative fusion peptide and corresponds with the previously described cleavage site within S2 (S2′) (40). Consistent with the class I fusion model, exemplified by influenza virus HA, trypsin cleavage at R890 would enable the bulky receptor binding head domain of the PEDV S protein to move aside, thereby liberating an N-terminal fusion peptide that can then insert into the host cell membrane to initiate membrane fusion (reviewed in reference 42).

In contrast to clinical PEDV isolates, entry by cell culture-adapted caPEDV into Vero cells is independent of trypsin. Yet, cell-cell fusion by infected cells still required the addition of trypsin, indicating that proteolysis activates the caDR13 S protein for fusion but does not occur at the plasma membrane. Candidate cellular enzymes that could activate the caPEDV S protein in the endolysosomal system are TTSPs and low-pH-activated proteases, similar to the activation of SARS-CoV, MERS-CoV, human coronavirus 229E, and MHV-2 S proteins (28, 43–46). Moreover, caPEDV infectivity was markedly affected by the action of trypsin, which correlated with a clear proteolysis of S proteins on virions. Trypsin cleavage of virion-bound Sca yielded a dominant 70-kDa-sized S2 fragment with an intact C terminus (Fig. 3B). The size of the product fits with trypsin cleavage in proximity to position G890 (i.e., at R885 or K889), yielding a truncated S2 subunit of approximately 70 kDa (predicted molecular mass of 55 kDa protein and 15 kDa *N*-glycans). We speculate that alternative trypsin cleavage sites may be more readily accessible in Sca compared to Swt and, hence, prematurely trigger the transition of Sca into a postfusion form. caPEDV has been used as a live attenuated vaccine, and its attenuated phenotype in pigs was suggested to be associated with a deletion in the accessory ORF3 gene product (39, 47, 48). We add that attenuation could also result from reduced viral fitness of the trypsin-independent PEDV vaccine strain in the gastric and pancreatic protease-rich environment of the intestine and by reduced syncytium-inflicted damage of the intestinal epithelial layer (41).

It seems counterintuitive that serial passaging of the trypsin-dependent PEDV-DR13 parental strain in the presence of trypsin eventually resulted in a cell culture-adapted caPEDV that no longer depended on trypsin for its growth (17). In fact, PEDV strain KPEDV-9 was independently generated by repeated passaging in cell culture (17, 39) and also acquired trypsin independence according to Park et al. (6). Intriguingly, it has been noted that Vero cells inhibit trypsin in cell culture supernatants by secretion of trypsin inhibitory molecules (49). Hence, propagation of the PEDV-DR13 parental strain in Vero cells may have selected for trypsin-independent PEDV mutants.

Comparing virus production in the presence and absence of trypsin, we also found that the release of recombinant viruses carrying wtPEDV and caPEDV S proteins from infected cells was increased by trypsin. Release of PEDV-Sca was 15-fold higher in the presence of trypsin, confirming results of Shirato et al. (22). PEDV-Swt was significantly more dependent on trypsin for release than PEDV-Sca, indicating that the S protein is also a determinant for efficient virus release from target cells. Protease activity acts at distinct steps in the viral life cycle of PEDV, although the mechanism of virus retention and the role of proteolysis in virus release are not understood.

Enveloped virus entry is generally directed and controlled by proteolytic processing of the fusion protein, receptor binding, and triggering of membrane fusion. Our knowledge about the determinants of PEDV infection is limited, and this study aimed at elucidating the requirements for virus entry. Like for other CoVs, we found that activating cleavage of wild-type PEDV S proteins occurs only after receptor binding (50). *In vitro*, PEDV is unique in its dependence on a protease that is not expressed by the target cell. As for influenza virus, this trypsin dependence may be an *ex vivo* requirement. *In vivo*, the availability of gastric and pancreatic proteases or proteases locally expressed by the intestinal epithelial target cells potentially mediate PEDV virus infection to the intestine (51). TTSPs such as TMPRSS2 are candidate proteases for PEDV activation, since human TMPRSS2 has been shown to activate PEDV S-mediated cell-cell fusion in cell culture (22). It is currently unknown whether PEDV S protein cleavage is a priming event and whether membrane fusion requires yet an additional trigger. So far, trypsin cleavage readily supports the membrane fusion process and can be used as a trigger to investigate virus-cell and cell-cell fusion and to dissect further details of the PEDV fusion machinery. Thus, it seems possible that PEDV infection is triggered by proteolysis rather than by alternative environmental cues, thereby abrogating the distinction between priming and triggering events, as was suggested for SARS-CoV (52).

ACKNOWLEDGMENTS

We acknowledge Zou Yong for kindly providing Vero cells. We thank Xander de Haan and Christine Burkard for helpful discussions during the design of this study.

This work was supported by E.C. 7th Framework Programme PITN-GA-2009-235649-Virus Entry and NWO MG (40-00506-98-12019).

REFERENCES

1. **Pensaert MB, de Bouck P.** 1978. A new coronavirus-like particle associated with diarrhea in swine. Arch. Virol. **58:**243–247. http://dx.doi.org/10.1007/BF01317606.
2. **AASV.** 2013. Porcine epidemic diarrhea information. American Association of Swine Veterinarians, Perry, IA.
3. **Li W, Li H, Liu Y, Pan Y, Deng F, Song Y, Tang X, He Q.** 2012. New variants of porcine epidemic diarrhea virus, China, 2011. Emerg. Infect. Dis. **18:**1350–1353. http://dx.doi.org/10.3201/eid1808.120002.
4. **Huang YW, Dickerman AW, Pineyro P, Li L, Fang L, Kiehne R, Opriessnig T, Meng XJ.** 2013. Origin, evolution, and genotyping of emergent porcine epidemic diarrhea virus strains in the United States. mBio **4**(5):e00737–13. http://dx.doi.org/10.1128/mBio.00737-13.
5. **Hofmann M, Wyler R.** 1988. Propagation of the virus of porcine epidemic diarrhea in cell culture. J. Clin. Microbiol. **26:**2235–2239.
6. **Park JE, Cruz DJ, Shin HJ.** 2011. Receptor-bound porcine epidemic diarrhea virus spike protein cleaved by trypsin induces membrane fusion. Arch. Virol. **156:**1749–1756. http://dx.doi.org/10.1007/s00705-011-1044-6.

7. **Duarte M, Tobler K, Bridgen A, Rasschaert D, Ackermann M, Laude H.** 1994. Sequence analysis of the porcine epidemic diarrhea virus genome between the nucleocapsid and spike protein genes reveals a polymorphic ORF. Virology **198:**466–476. http://dx.doi.org/10.1006/viro.1994.1058.
8. **Bosch BJ, van der Zee R, de Haan CA, Rottier PJ.** 2003. The coronavirus spike protein is a class I virus fusion protein: structural and functional characterization of the fusion core complex. J. Virol. **77:**8801–8811. http://dx.doi.org/10.1128/JVI.77.16.8801-8811.2003.
9. **White JM, Delos SE, Brecher M, Schornberg K.** 2008. Structures and mechanisms of viral membrane fusion proteins: multiple variations on a common theme. Crit. Rev. Biochem. Mol. Biol. **43:**189–219. http://dx.doi.org/10.1080/10409230802058320.
10. **Frana MF, Behnke JN, Sturman LS, Holmes KV.** 1985. Proteolytic cleavage of the E2 glycoprotein of murine coronavirus: host-dependent differences in proteolytic cleavage and cell fusion. J. Virol. **56:**912–920.
11. **Cavanagh D.** 1983. Coronavirus IBV: structural characterization of the spike protein. J. Gen. Virol. **64**(Part 12)**:**2577–2583.
12. **Xiao X, Chakraborti S, Dimitrov AS, Gramatikoff K, Dimitrov DS.** 2003. The SARS-CoV S glycoprotein: expression and functional characterization. Biochem. Biophys. Res. Commun. **312:**1159–1164. http://dx.doi.org/10.1016/j.bbrc.2003.11.054.
13. **Watanabe R, Matsuyama S, Shirato K, Maejima M, Fukushi S, Morikawa S, Taguchi F.** 2008. Entry from the cell surface of severe acute respiratory syndrome coronavirus with cleaved S protein as revealed by pseudotype virus bearing cleaved S protein. J. Virol. **82:**11985–11991. http://dx.doi.org/10.1128/JVI.01412-08.
14. **Yamada Y, Liu DX.** 2009. Proteolytic activation of the spike protein at a novel RRRR/S motif is implicated in furin-dependent entry, syncytium formation, and infectivity of coronavirus infectious bronchitis virus in cultured cells. J. Virol. **83:**8744–8758. http://dx.doi.org/10.1128/JVI.00613-09.
15. **Matsuyama S, Taguchi F.** 2002. Receptor-induced conformational changes of murine coronavirus spike protein. J. Virol. **76:**11819–11826. http://dx.doi.org/10.1128/JVI.76.23.11819-11826.2002.
16. **Li C, Li Z, Zou Y, Wicht O, van Kuppeveld FJ, Rottier PJ, Bosch BJ.** 2013. Manipulation of the porcine epidemic diarrhea virus genome using targeted RNA recombination. PLoS One **8:**e69997. http://dx.doi.org/10.1371/journal.pone.0069997.
17. **Song DS, Yang JS, Oh JS, Han JH, Park BK.** 2003. Differentiation of a Vero cell adapted porcine epidemic diarrhea virus from Korean field strains by restriction fragment length polymorphism analysis of ORF 3. Vaccine **21:**1833–1842. http://dx.doi.org/10.1016/S0264-410X(03)00027-6.
18. **Egberink HF, Ederveen J, Callebaut P, Horzinek MC.** 1988. Characterization of the structural proteins of porcine epizootic diarrhea virus, strain CV777. Am. J. Vet. Res. **49:**1320–1324.
19. **Rossen JW, Bekker CP, Strous GJ, Horzinek MC, Dveksler GS, Holmes KV, Rottier PJ.** 1996. A murine and a porcine coronavirus are released from opposite surfaces of the same epithelial cells. Virology **224:**345–351. http://dx.doi.org/10.1006/viro.1996.0540.
20. **Park SJ, Moon HJ, Yang JS, Lee CS, Song DS, Kang BK, Park BK.** 2007. Sequence analysis of the partial spike glycoprotein gene of porcine epidemic diarrhea viruses isolated in Korea. Virus Genes **35:**321–332. http://dx.doi.org/10.1007/s11262-007-0096-x.
21. **Shirato K, Maejima M, Matsuyama S, Ujike M, Miyazaki A, Takeyama N, Ikeda H, Taguchi F.** 2011. Mutation in the cytoplasmic retrieval signal of porcine epidemic diarrhea virus spike (S) protein is responsible for enhanced fusion activity. Virus Res. **161:**188–193. http://dx.doi.org/10.1016/j.virusres.2011.07.019.
22. **Shirato K, Matsuyama S, Ujike M, Taguchi F.** 2011. Role of proteases in the release of porcine epidemic diarrhea virus from infected cells. J. Virol. **85:**7872–7880. http://dx.doi.org/10.1128/JVI.00464-11.
23. **Kido H, Okumura Y, Takahashi E, Pan HY, Wang S, Chida J, Le TQ, Yano M.** 2008. Host envelope glycoprotein processing proteases are indispensable for entry into human cells by seasonal and highly pathogenic avian influenza viruses. J. Mol. Genet. Med. **3:**167–175.
24. **Kantanen ML, Leinikki P, Kuismanen E.** 1995. Endoproteolytic cleavage of HIV-1 gp160 envelope precursor occurs after exit from the trans-Golgi network (TGN). Arch. Virol. **140:**1441–1449. http://dx.doi.org/10.1007/BF01322670.
25. **Bugge TH, Antalis TM, Wu Q.** 2009. Type II transmembrane serine proteases. J. Biol. Chem. **284:**23177–23181. http://dx.doi.org/10.1074/jbc.R109.021006.
26. **Bottcher E, Matrosovich T, Beyerle M, Klenk HD, Garten W, Matrosovich M.** 2006. Proteolytic activation of influenza viruses by serine proteases TMPRSS2 and HAT from human airway epithelium. J. Virol. **80:**9896–9898. http://dx.doi.org/10.1128/JVI.01118-06.
27. **Simmons G, Gosalia DN, Rennekamp AJ, Reeves JD, Diamond SL, Bates P.** 2005. Inhibitors of cathepsin L prevent severe acute respiratory syndrome coronavirus entry. Proc. Natl. Acad. Sci. U. S. A. **102:**11876–11881. http://dx.doi.org/10.1073/pnas.0505577102.
28. **Matsuyama S, Nagata N, Shirato K, Kawase M, Takeda M, Taguchi F.** 2010. Efficient activation of the severe acute respiratory syndrome coronavirus spike protein by the transmembrane protease TMPRSS2. J. Virol. **84:**12658–12664. http://dx.doi.org/10.1128/JVI.01542-10.
29. **Krzyzaniak MA, Zumstein MT, Gerez JA, Picotti P, Helenius A.** 2013. Host cell entry of respiratory syncytial virus involves macropinocytosis followed by proteolytic activation of the F protein. PLoS Pathog. **9:**e1003309. http://dx.doi.org/10.1371/journal.ppat.1003309.
30. **Belouzard S, Chu VC, Whittaker GR.** 2009. Activation of the SARS coronavirus spike protein via sequential proteolytic cleavage at two distinct sites. Proc. Natl. Acad. Sci. U. S. A. **106:**5871–5876. http://dx.doi.org/10.1073/pnas.0809524106.
31. **Matsuyama S, Taguchi F.** 2009. Two-step conformational changes in a coronavirus envelope glycoprotein mediated by receptor binding and proteolysis. J. Virol. **83:**11133–11141. http://dx.doi.org/10.1128/JVI.00959-09.
32. **Li BX, Ge JW, Li YJ.** 2007. Porcine aminopeptidase N is a functional receptor for the PEDV coronavirus. Virology **365:**166–172. http://dx.doi.org/10.1016/j.virol.2007.03.031.
33. **Bertram S, Dijkman R, Habjan M, Heurich A, Gierer S, Glowacka I, Welsch K, Winkler M, Schneider H, Hofmann-Winkler H, Thiel V, Pohlmann S.** 2013. TMPRSS2 activates the human coronavirus 229E for cathepsin-independent host cell entry and is expressed in viral target cells in the respiratory epithelium. J. Virol. **87:**6150–6160. http://dx.doi.org/10.1128/JVI.03372-12.
34. **Bertram S, Heurich A, Lavender H, Gierer S, Danisch S, Perin P, Lucas JM, Nelson PS, Pohlmann S, Soilleux EJ.** 2012. Influenza and SARS-coronavirus activating proteases TMPRSS2 and HAT are expressed at multiple sites in human respiratory and gastrointestinal tracts. PLoS One **7:**e35876. http://dx.doi.org/10.1371/journal.pone.0035876.
35. **Licitra BN, Millet JK, Regan AD, Hamilton BS, Rinaldi VD, Duhamel GE, Whittaker GR.** 2013. Mutation in spike protein cleavage site and pathogenesis of feline coronavirus. Emerg. Infect. Dis. **19:**1066–1073. http://dx.doi.org/10.3201/eid1907.121094.
36. **Kido H, Okumura Y, Takahashi E, Pan HY, Wang S, Yao D, Yao M, Chida J, Yano M.** 2012. Role of host cellular proteases in the pathogenesis of influenza and influenza-induced multiple organ failure. Biochim. Biophys. Acta **1824:**186–194. http://dx.doi.org/10.1016/j.bbapap.2011.07.001.
37. **Tay FP, Huang M, Wang L, Yamada Y, Liu DX.** 2012. Characterization of cellular furin content as a potential factor determining the susceptibility of cultured human and animal cells to coronavirus infectious bronchitis virus infection. Virology **433:**421–430. http://dx.doi.org/10.1016/j.virol.2012.08.037.
38. **Baker M, Prasad BV.** 2010. Rotavirus cell entry. Curr. Top. Microbiol. Immunol. **343:**121–148. http://dx.doi.org/10.1007/82_2010_34.
39. **Kweon CH, Kwon BJ, Lee JG, Kwon GO, Kang YB.** 1999. Derivation of attenuated porcine epidemic diarrhea virus (PEDV) as vaccine candidate. Vaccine **17:**2546–2553. http://dx.doi.org/10.1016/S0264-410X(99)00059-6.
40. **Madu IG, Roth SL, Belouzard S, Whittaker GR.** 2009. Characterization of a highly conserved domain within the severe acute respiratory syndrome coronavirus spike protein S2 domain with characteristics of a viral fusion peptide. J. Virol. **83:**7411–7421. http://dx.doi.org/10.1128/JVI.00079-09.
41. **Park SJ, Song DS, Ha GW, Park BK.** 2007. Cloning and further sequence analysis of the spike gene of attenuated porcine epidemic diarrhea virus DR13. Virus Genes **35:**55–64. http://dx.doi.org/10.1007/s11262-006-0036-1.
42. **Harrison SC.** 2008. Viral membrane fusion. Nat. Struct. Mol. Biol. **15:**690–698. http://dx.doi.org/10.1038/nsmb.1456.
43. **Qiu Z, Hingley ST, Simmons G, Yu C, Das Sarma J, Bates P, Weiss SR.** 2006. Endosomal proteolysis by cathepsins is necessary for murine coronavirus mouse hepatitis virus type 2 spike-mediated entry. J. Virol. **80:**5768–5776. http://dx.doi.org/10.1128/JVI.00442-06.
44. **Huang IC, Bosch BJ, Li F, Li W, Lee KH, Ghiran S, Vasilieva N,**

Dermody TS, Harrison SC, Dormitzer PR, Farzan M, Rottier PJ, Choe H. 2006. SARS coronavirus, but not human coronavirus NL63, utilizes cathepsin L to infect ACE2-expressing cells. J. Biol. Chem. **281:**3198–3203. http://dx.doi.org/10.1074/jbc.M508381200.

45. **Kawase M, Shirato K, Matsuyama S, Taguchi F.** 2009. Protease-mediated entry via the endosome of human coronavirus 229E. J. Virol. **83:**712–721. http://dx.doi.org/10.1128/JVI.01933-08.
46. **Gierer S, Bertram S, Kaup F, Wrensch F, Heurich A, Kramer-Kuhl A, Welsch K, Winkler M, Meyer B, Drosten C, Dittmer U, von Hahn T, Simmons G, Hofmann H, Pohlmann S.** 2013. The spike protein of the emerging betacoronavirus EMC uses a novel coronavirus receptor for entry, can be activated by TMPRSS2, and is targeted by neutralizing antibodies. J. Virol. **87:**5502–5511. http://dx.doi.org/10.1128/JVI.00128-13.
47. **Sato T, Takeyama N, Katsumata A, Tuchiya K, Kodama T, Kusanagi K.** 2011. Mutations in the spike gene of porcine epidemic diarrhea virus associated with growth adaptation *in vitro* and attenuation of virulence *in vivo*. Virus Genes **43:**72–78. http://dx.doi.org/10.1007/s11262-011-0617-5.
48. **Park SJ, Moon HJ, Luo Y, Kim HK, Kim EM, Yang JS, Song DS, Kang BK, Lee CS, Park BK.** 2008. Cloning and further sequence analysis of the ORF3 gene of wild- and attenuated-type porcine epidemic diarrhea viruses. Virus Genes **36:**95–104. http://dx.doi.org/10.1007/s11262-007-0164-2.
49. **Kaverin NV, Webster RG.** 1995. Impairment of multicycle influenza virus growth in Vero (WHO) cells by loss of trypsin activity. J. Virol. **69:**2700–2703.
50. **Belouzard S, Millet JK, Licitra BN, Whittaker GR.** 2012. Mechanisms of coronavirus cell entry mediated by the viral spike protein. Viruses **4:**1011–1033. http://dx.doi.org/10.3390/v4061011.
51. **Zamolodchikova TS.** 2012. Serine proteases of small intestine mucosa—localization, functional properties, and physiological role. Biochemistry **77:**820–829. http://dx.doi.org/10.1134/S0006297912080032.
52. **Simmons G, Zmora P, Gierer S, Heurich A, Pohlmann S.** 2013. Proteolytic activation of the SARS-coronavirus spike protein: cutting enzymes at the cutting edge of antiviral research. Antiviral Res. **100:**605–614. http://dx.doi.org/10.1016/j.antiviral.2013.09.028.